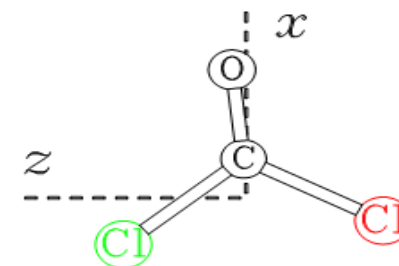
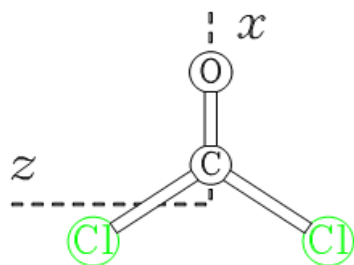


FIRST HIGH-RESOLUTION ANALYSIS OF PHOSGENE $^{35}\text{Cl}_2\text{CO}$ AND $^{35}\text{Cl}^{37}\text{ClCO}$ FUNDAMENTALS IN THE 250 - 480 CM^{-1} SPECTRAL REGION



**F. Kwabia Tchana¹, M. Ndao¹, L. Manceron², A. Perrin¹,
J. M. Flaud¹, W.J. Lafferty³**

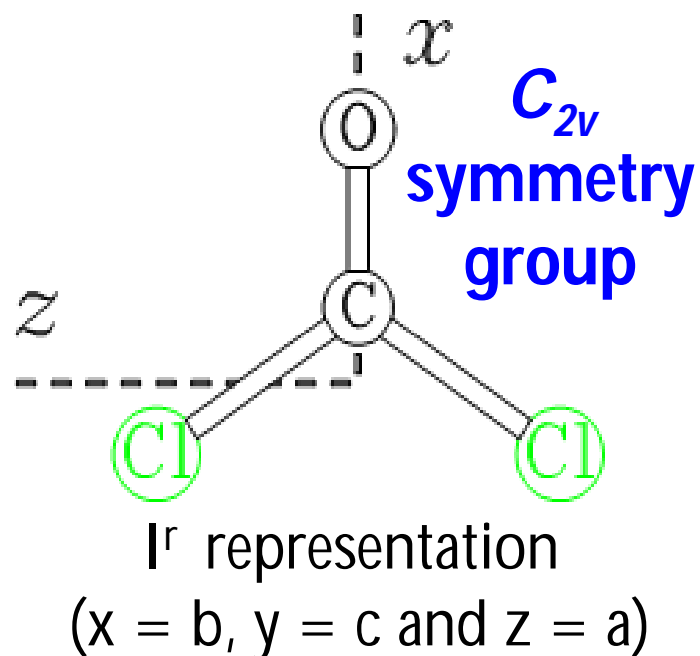
¹Laboratoire Interuniversitaire des Systèmes Atmosphériques, UMR CNRS 7583, Université Paris Diderot, France

²Ligne AILES, Synchrotron SOLEIL and MONARIS, CNRS UMR 8233, Université Pierre et Marie Curie, France

³Sensor Science Division, National Institute of Standards and Technology, USA



Modes of vibration of phosgene $^{35}\text{Cl}_2\text{CO}$



A_1	A_2	B_1	B_2
ν_1 (1827 cm^{-1})		ν_4 (580 cm^{-1})	ν_5 (849 cm^{-1})
	ν_2 (567 cm^{-1})		ν_6 (440 cm^{-1})
	ν_3 (285 cm^{-1})		

Phosgene has **6 IR** modes, **2** in the mid-infrared (ν_1 and ν_5) and **4 low energy modes**: ν_3 , ν_6 , ν_2 and ν_4

➔ **Lots of strong hot bands in the 11.8 μm spectral region where the phosgene is detected and modelled**

These hot bands complicate the analysis of spectra !!

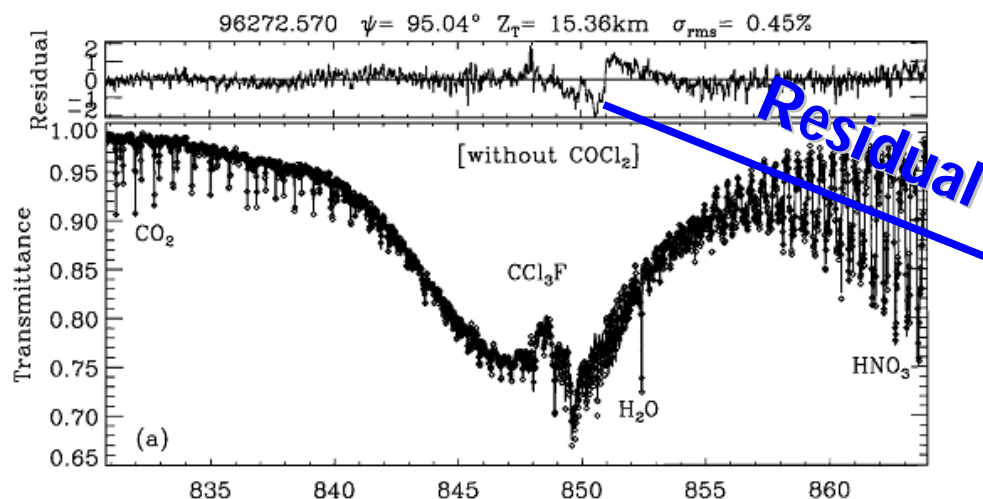
Detection of atmospheric Cl_2CO : Use of the atmospheric window around $11\ \mu\text{m}$

- **Phosgene is relatively more abundant in the stratosphere**, where it has a lifetime of several years, **but is also present in the troposphere** in spite of a shorter lifetime (**seventy days**)
- Strong infrared absorption of phosgene (ν_5) occur in the same spectral region ($850\ \text{cm}^{-1}/11.8\ \mu\text{m}$) as **Freon-11 (CCl_3F)**, **which leads to an overestimation of the concentration of Freon-11, if one does not take into account the absorption of phosgene as can be seen on the residual of this figure**

\$ Toon et al., *Geophys. Res. Lett.*, **28** (2001) 2835

Detection of atmospheric Cl_2CO : Use of the atmospheric window around $11\ \mu\text{m}$

- Phosgene is relatively more abundant in the stratosphere, where it has a lifetime of several years, but is also present in the troposphere in spite of a shorter lifetime (seventy days)
- Strong infrared absorption of phosgene (ν_5) occur in the same spectral region ($850\ \text{cm}^{-1}/11.8\ \mu\text{m}$) as Freon-11 (CCl_3F), which leads to an overestimation of the concentration of Freon-11, if one does not take into account the absorption of phosgene as can be seen on the residual of this figure

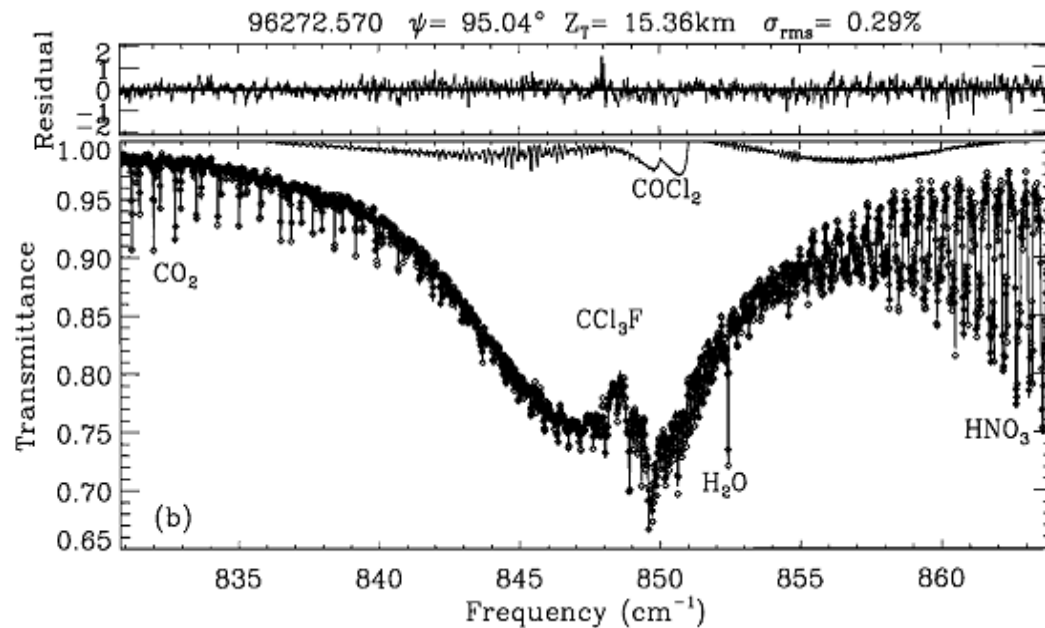


Spectral fit to a MkIV limb transmittance spectrum at 15.36 km tangent altitude performed without absorption of the ν_5 band of atmospheric Cl_2CO

§ Toon et al., *Geophys. Res. Lett.*, **28** (2001) 2835

Modelling of atmospheric Cl_2CO :

Performed with a linelist simulating the absorption of the ν_5 band of atmospheric Cl_2CO

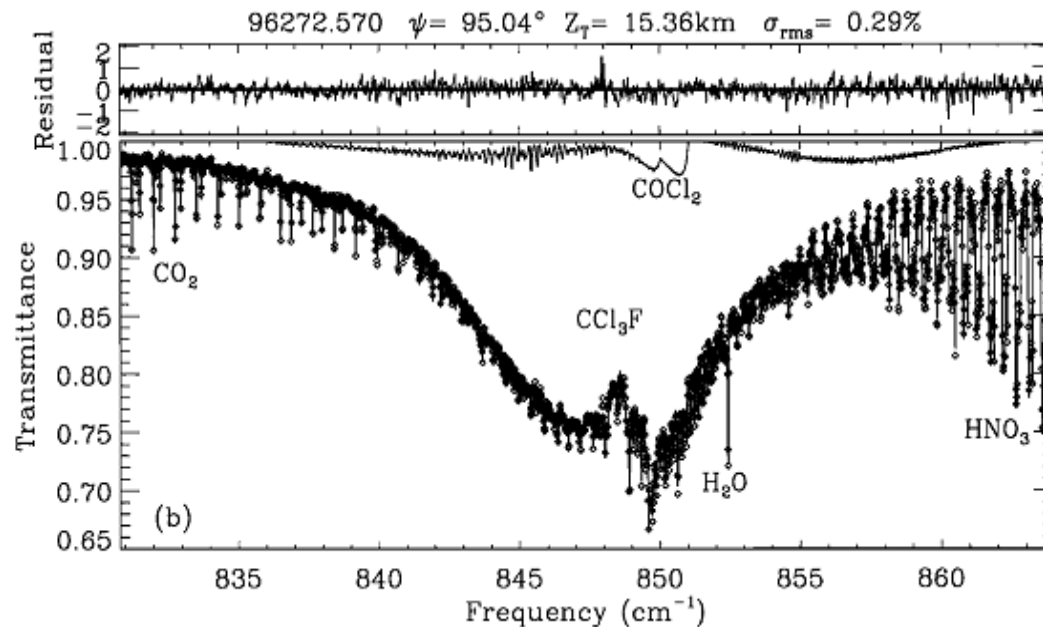


Precise modelling of phosgene absorptions in this infrared atmospheric windows requires the study of the ν_5 band **but also the low vibrational energy such as: ν_3 (285 cm^{-1}) and ν_6 (440 cm^{-1}) bands.**

Toon et al., *Geophys. Res. Lett.*, **28** (2001) 2835

Modelling of atmospheric Cl_2CO :

Performed with a linelist simulating the absorption of the ν_5 band of atmospheric Cl_2CO



The omission of these hot bands leads to a systematic error of more than 20% in the retrieved profiles.

Toon et al., *Geophys. Res. Lett.*, **28** (2001) 2835

Precise modelling of phosgene absorptions in this infrared atmospheric windows requires the study of the ν_5 band **but also the low vibrational energy such as: ν_3 (285 cm^{-1}) and ν_6 (440 cm^{-1}) bands.**

Indeed these far infrared fundamentals are responsible for **hot bands ($\nu_5 + \nu_3 - \nu_3$ and $\nu_5 + \nu_6 - \nu_6, \dots$)**, not analysed but of great importance for the correct retrieval of Freon-11.

Previous study

- **Microwave spectra: determination of phosgene structure and ground state parameters**

Wilse and Robinson, *J. Chem. Phys.* **21** (1953) 1741

Mirri et al., *Spectro. Chem. Acta A* **27** (1971) 937

Carpenter and Rimmer, *J. Chem. Soc. Faraday Trans. 2* **74** (1978) 466

Nakata et al., *J. Mol. Spectrosc.* **83** (1980) 105

Nakata et al., *J. Mol. Spectrosc.* **83** (1980) 118

- **Tunable diode laser spectrum: very partial study of the strong ν_1 and ν_5 bands**

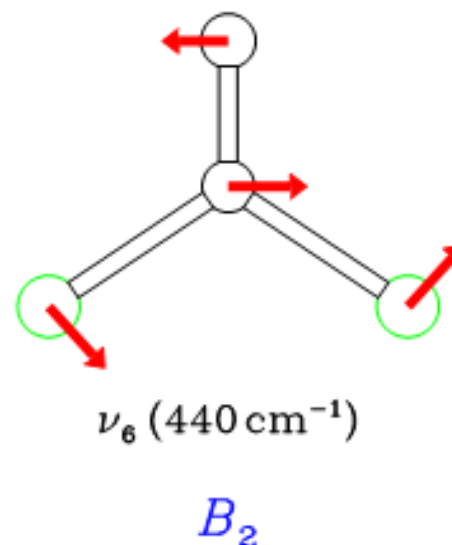
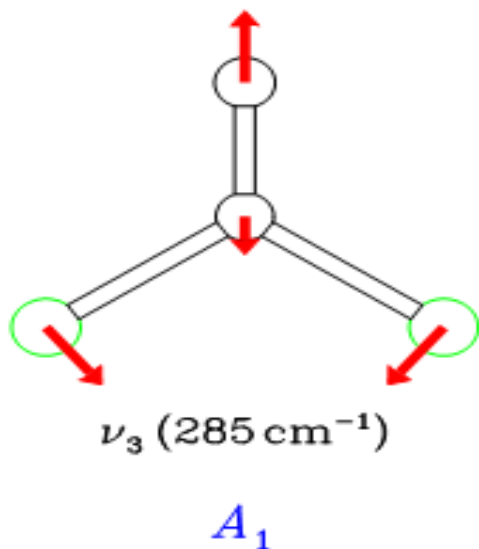
Yamamoto et al., *J. Mol. Spectrosc.* **106** (1984) 376

- **High resolution Fourier transform spectra: detailed and extensive analysis of the strong ν_1 and ν_5 bands**

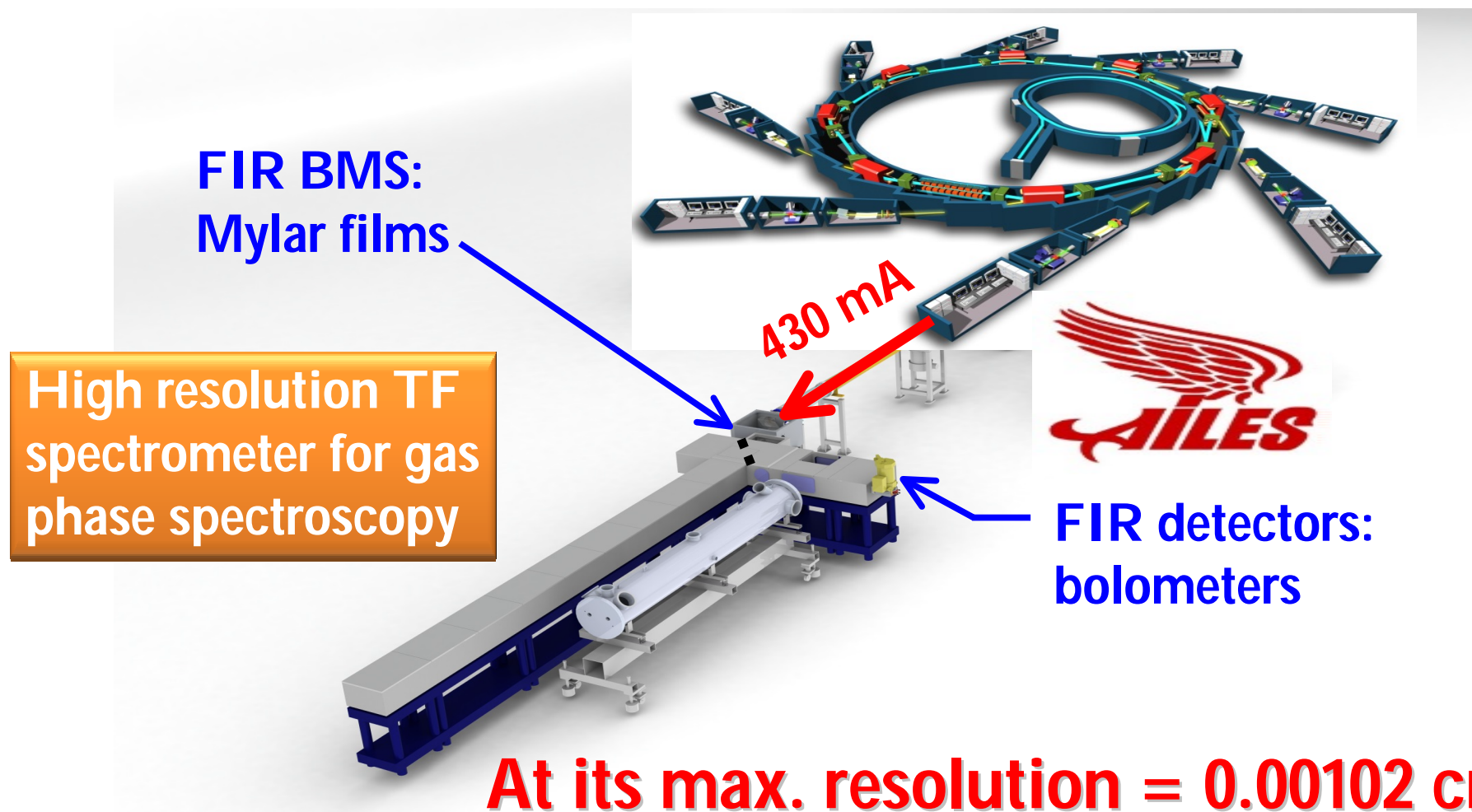
Kwabia Tchana et al., *Molecular Physics* **113** (2015) 3241

Present study

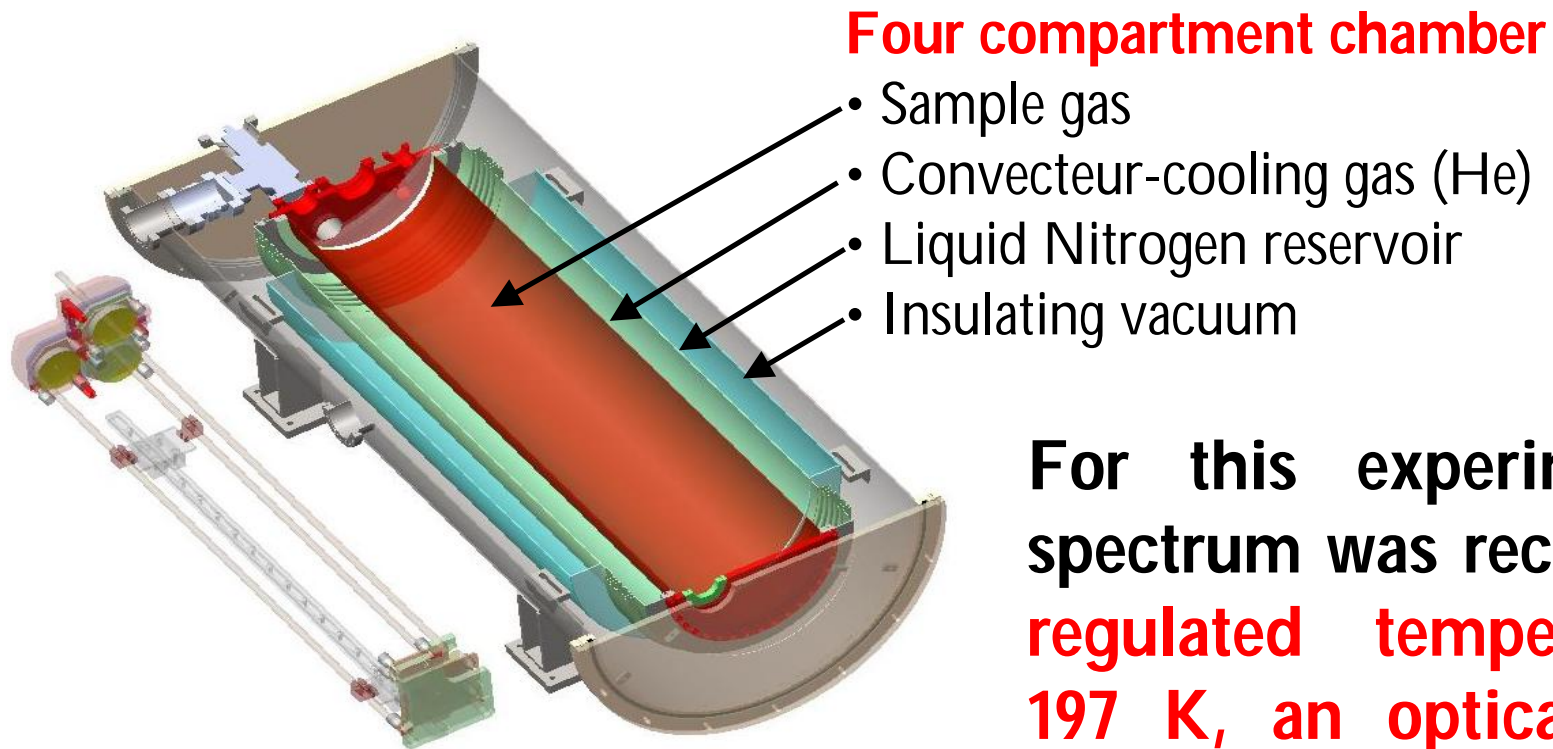
- We recorded the **high resolution** (0.00102 cm^{-1}) FT far-infrared spectra of phosgene: $^{35}\text{Cl}_2\text{CO}$ (57%), $^{35}\text{Cl}^{37}\text{ClCO}$ (37%) and $^{37}\text{Cl}_2\text{CO}$ (6%)
- First line position analysis of the ν_3 (285 cm^{-1}) and ν_6 (440 cm^{-1}) bands of the most abundant isotopomers $^{35}\text{Cl}_2\text{CO}$ and $^{35}\text{Cl}^{37}\text{ClCO}$



Experimental setup: Synchrotron source coupled to the high resolution Fourier transform spectrometer and long-path cryogenic cell



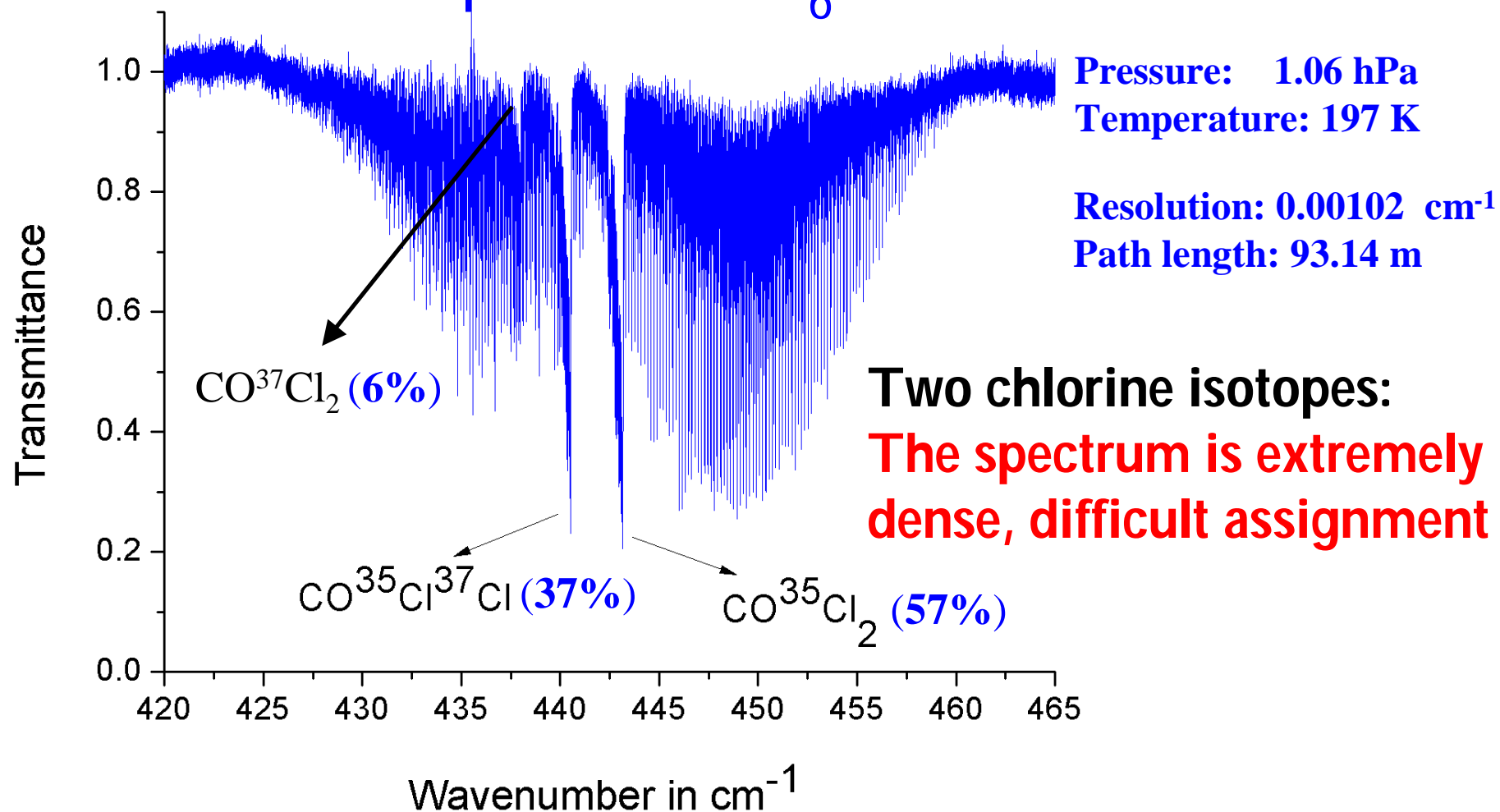
Experimental setup: Synchrotron source coupled to the high resolution Fourier transform spectrometer and **long-path cryogenic cell**



For this experiment, the spectrum was recorded at a **regulated temperature of 197 K**, an optical path of **93.14 m** and phosgene pressure of **1.06 hPa**

High resolution FT spectra of the ν_3 and ν_6 bands of $^{35}\text{Cl}_2\text{CO}$, $^{35}\text{Cl}^{37}\text{ClCO}$ and $^{37}\text{Cl}_2\text{CO}$

Example of the ν_6 bands



Watson-type Hamiltonian used to calculate the upper states ro-vibrational 3^1 and 6^1 of phosgene

The upper state rotational constants were obtained using a **Watson A-type Hamiltonian written in the I^r representation ($x = b$, $y = c$ and $z = a$)**

$$\begin{aligned} H_W = & E_v + \left[A^v - \frac{1}{2}(B^v + C^v) \right] J_z^2 + \frac{1}{2}(B^v + C^v) J^2 + \frac{1}{2}(B^v - C^v) J_{xy}^2 \\ & - \Delta_K^v J_z^4 - \Delta_{JK}^v J_z^2 J^2 - \Delta_J^v (J^2)^2 - \delta_K^v \{ J_z^2, J_{xy}^2 \} - 2\delta_J^v J_{xy}^2 J^2 \\ & + H_K^v J_z^6 + H_{KJ}^v J_z^4 J^2 + H_{JK}^v J_z^2 (J^2)^2 + H_J^v (J^2)^3 \\ & + h_K^v \{ J_z^4, J_{xy}^2 \} + h_{KJ}^v \{ J_z^2, J_{xy}^2 \} J^2 + 2h_J^v J_{xy}^2 (J^2)^2 + \dots \end{aligned}$$

Energy level is defined by the quantum numbers J , K_a and K_c

$$0 \leq K_a \leq J, 0 \leq K_c \leq J, K_a + K_c = J \text{ or } J + 1$$

Results of the fit for the ν_3 bands of $^{35}\text{Cl}_2\text{CO}$ and $^{35}\text{Cl}^{37}\text{ClCO}$

Range of quantum numbers observed for experimental energy levels, number of lines and RMS of the vibrational state $\nu_3 = 1$

Isotopomers	J range	K_a range	No. of lines	RMS (cm^{-1})
$^{35}\text{Cl}_2\text{CO}$	2-78	0-41	5032	0.00021
$^{35}\text{Cl}^{37}\text{ClCO}$	2-75	0-41	4634	0.00038

For the two isotopomers we have reproduced **more than 9000 transitions** ($J_{\text{max}} = 78$, $K_{\text{amax}} = 41$), with an **RMS better than 0.0004 cm^{-1}**

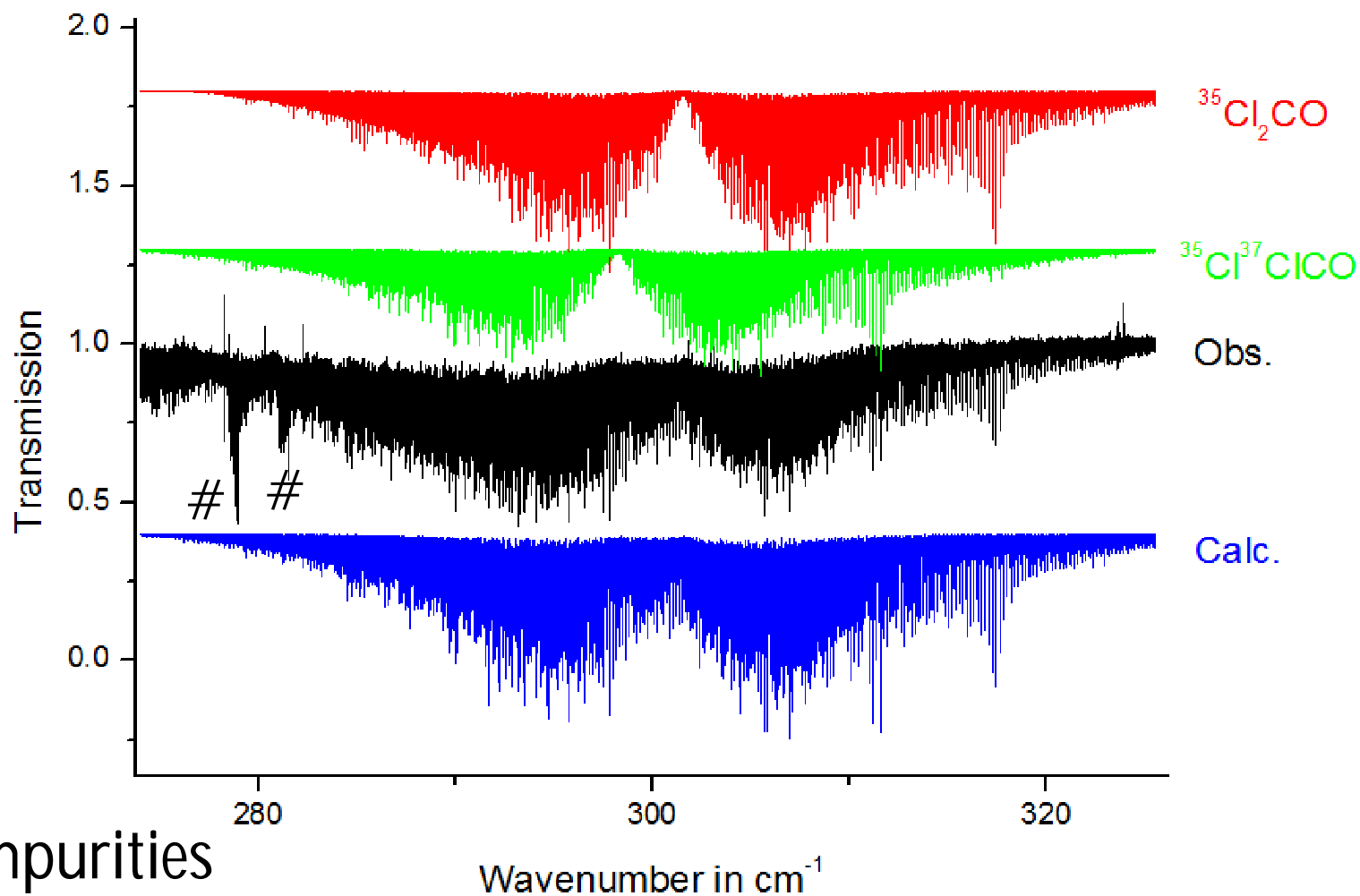
Results of the fit for the ν_6 bands of $^{35}\text{Cl}_2\text{CO}$ and $^{35}\text{Cl}^{37}\text{ClCO}$

Range of quantum numbers observed for experimental energy levels, number of lines and RMS of the vibrational state $\nu_6 = 1$

Isotopomers	J range	K_a range	No. of lines	RMS (cm^{-1})
$^{35}\text{Cl}_2\text{CO}$	2-77	0-34	4846	0.00030
$^{35}\text{Cl}^{37}\text{ClCO}$	2-71	0-33	4250	0.00043

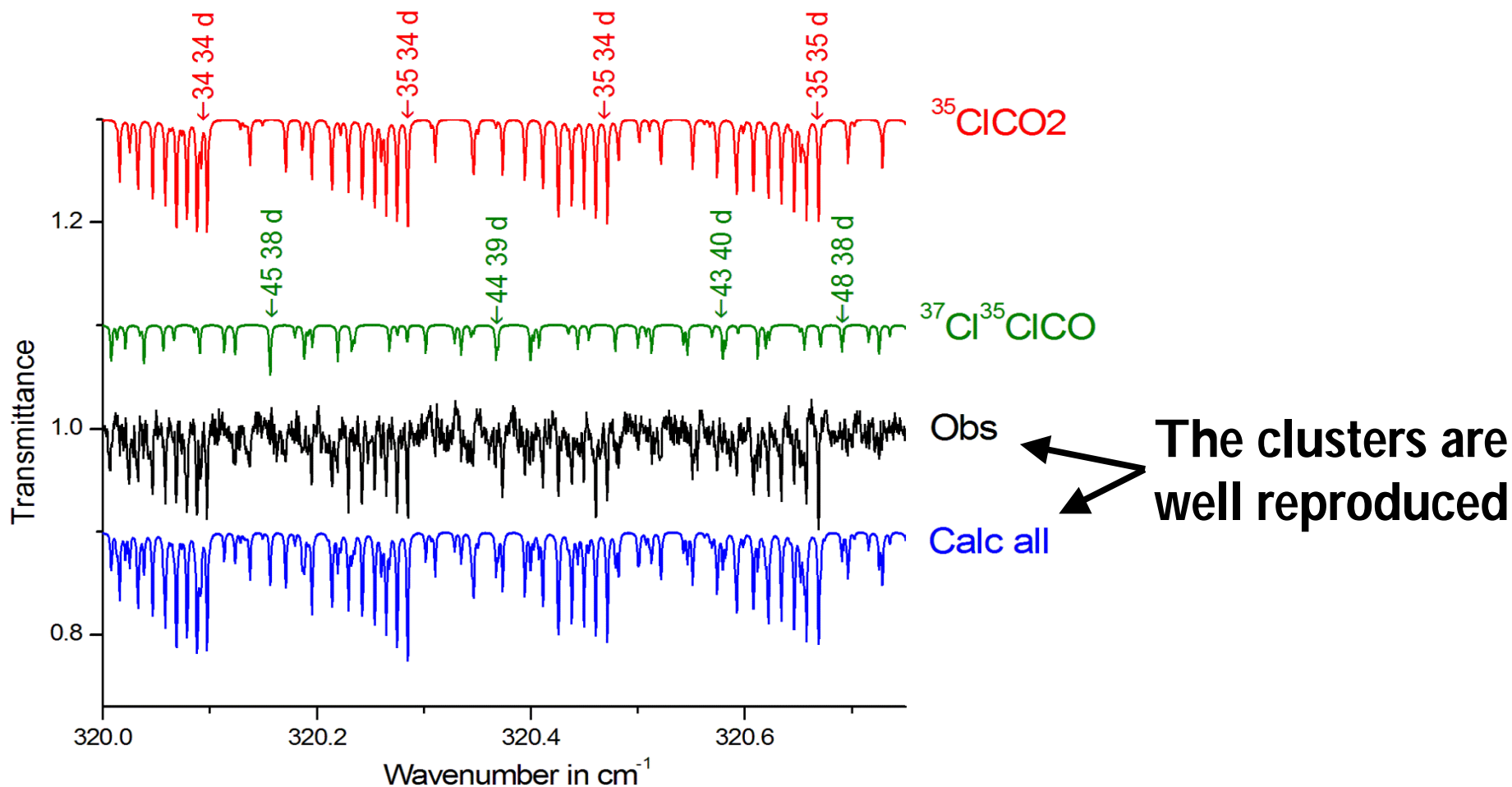
For the two isotopomers we have reproduced **more than 9000 transitions** ($J_{\text{max}} = 77$, $K_{\text{amax}} = 34$), with an **RMS better than 0.00045 cm^{-1}**

Comparison of spectra: observed and simulated spectra, ν_3 band of Cl_2CO

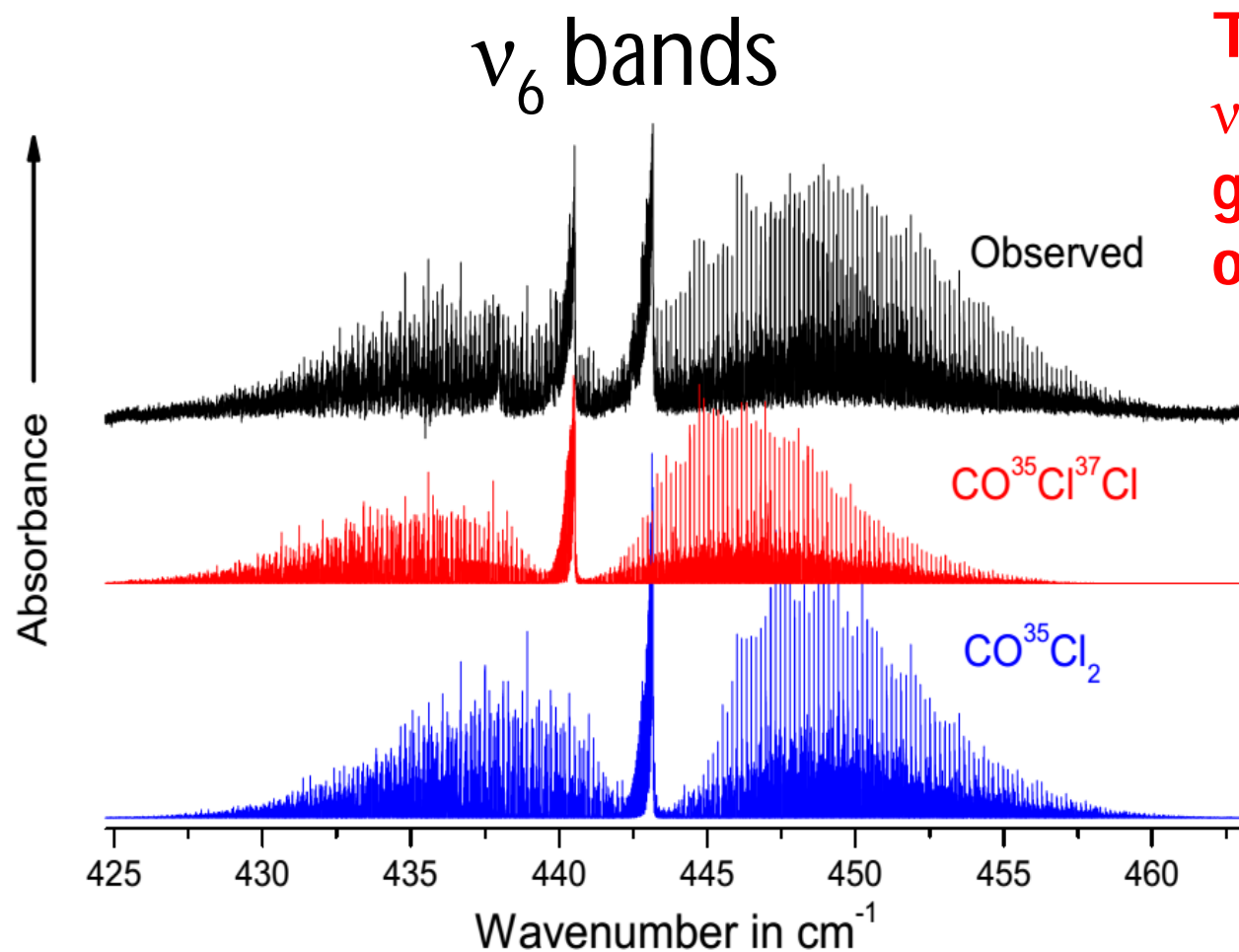


Impurities

Portion of the R-branches of the ν_3 bands of $^{35}\text{Cl}_2\text{CO}$ and $^{35}\text{Cl}^{37}\text{ClCO}$



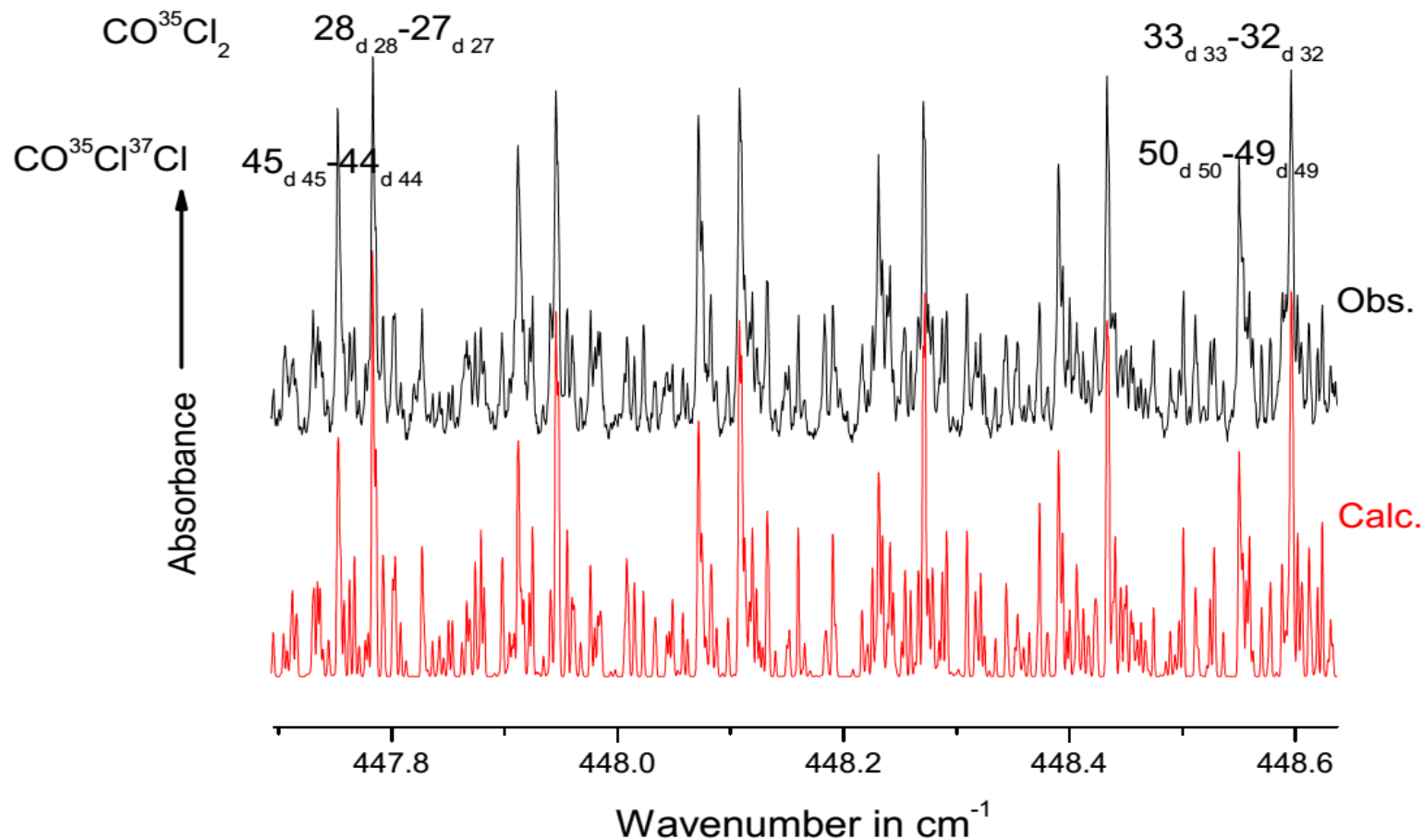
Comparison of spectra: observed and simulated spectra, ν_6 band of Cl_2CO



The simulation of the ν_6 band also shows a good agreement with observation

The distinctive shape of the two A-type bands ν_6 of $^{35}\text{Cl}_2\text{CO}$ and $^{35}\text{Cl}^{37}\text{ClCO}$ with their narrow Q-branches are clearly recognizable.

Portion of the R-branches of the ν_6 bands of $^{35}\text{Cl}_2\text{CO}$ and $^{35}\text{Cl}^{37}\text{ClCO}$



The good agreement between observation and simulation demonstrates the quality of the analysis and the fitting

Conclusions and Outlook

- First high-resolution infrared absorption spectra of Cl_2CO isotopomers: $^{35}\text{Cl}_2\text{CO}$ and $^{35}\text{Cl}^{37}\text{ClCO}$ between 250 to 480 cm^{-1} .
- First determination of the upper-state rotational and distortion constants for ν_3 and ν_6 bands.
- We also recorded the ν_2 (567 cm^{-1}) and ν_4 (580 cm^{-1}) bands of $^{35}\text{Cl}_2\text{CO}$ and $^{35}\text{Cl}^{37}\text{ClCO}$. The analysis of these two bands is in progress.
- **Outlook:** Study the hot bands, measuring the intensities and the widths of the mid-infrared band of Cl_2CO as a function of temperature. This is important for solving the 40 % discrepancies between the existing room temperature measurements, and to clarify the contribution of hot bands.
- **Objective:** Provide full prediction including intensities and linewidths for remote sensing in the 11.8 μm spectral region.

END

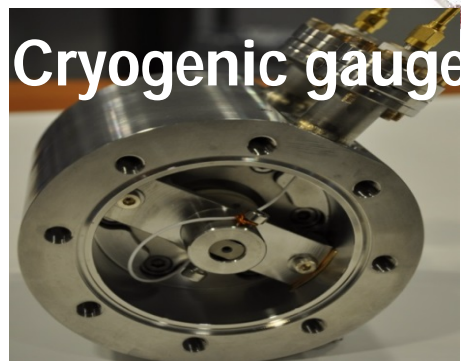
Thanks you for your attention!!

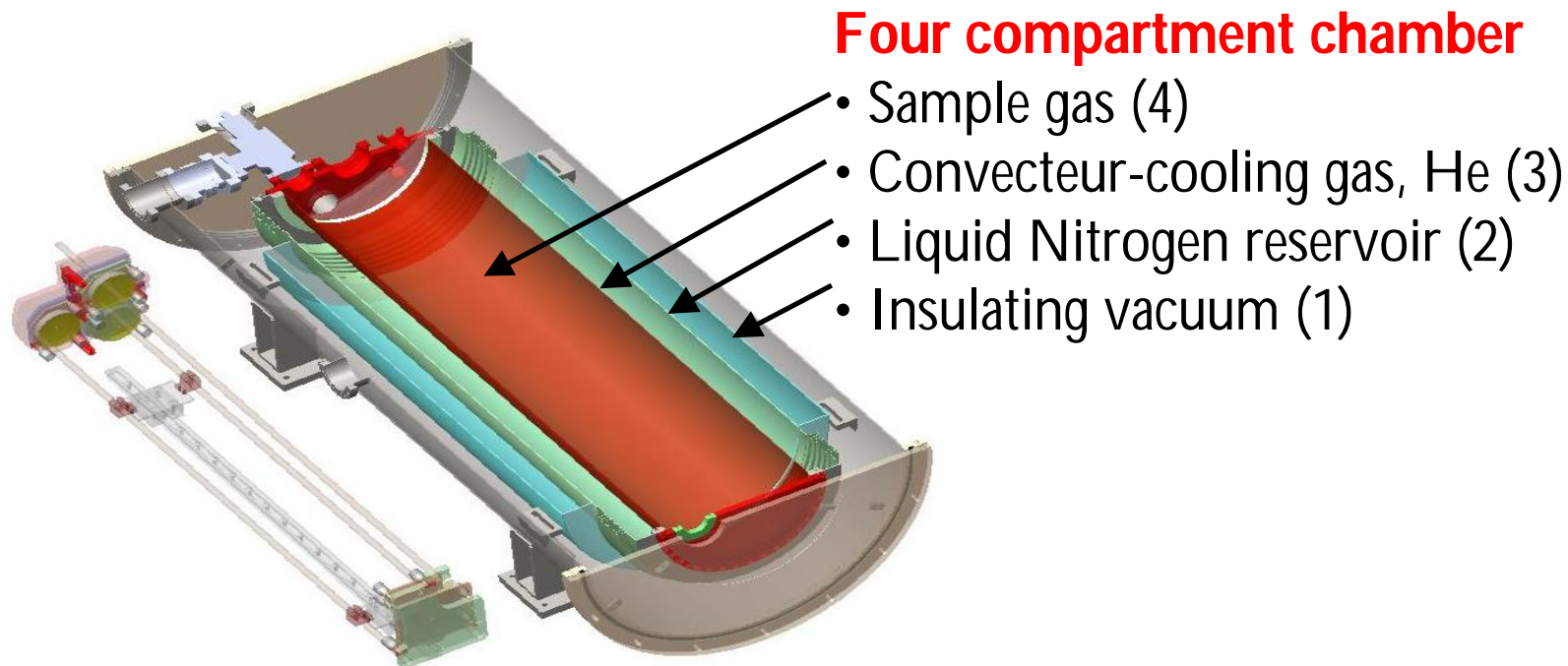
Specifications of the LISA-SOLEIL long-path cryogenic cell

Four compartment chamber

- Sample gas (4)
- Convecteur-cooling gas, He (3)
- Liquid Nitrogen reservoir (2)
- Insulating vacuum (1)

- Variable optical path :
3 to more than 141 m
- Spectral range **10 to 4000 cm^{-1}**
- Temperature adjustable in the
80 to 400 K range, within ± 2 K
- Cryogenic gauge **0.2 to 40 mb**,
measured with ± 1 %



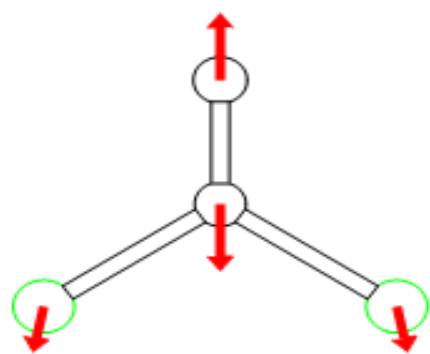


We chose a concept with a completely static configuration (no forced circulation pump, no closed cycle cooler) including a large cryostat around the cell body and additional gas convection cooling. The cooling power originates from the heat of vaporization of liquid nitrogen, giving off approximately 69 W of cooling power per liter of liquid nitrogen evaporated per hour, even at the lowest temperature, and thus keeping chamber 2 at a constant 77 K temperature. The heat is transmitted through radiative cooling to the inner envelopes or, more efficiently, through convection by filling the chamber 3 with helium gas. The helium pressure can be varied to adapt the cooling power to the desired end temperature.

Atmospheric Cl_2CO

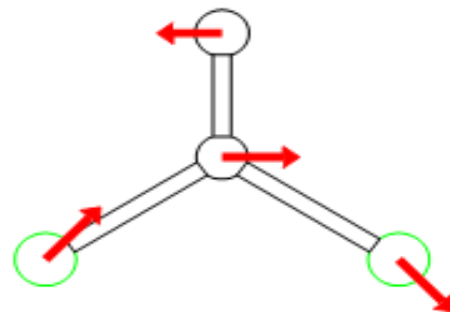
Atmospheric COCl_2 is formed from the breakdown of chlorinated hydrocarbons such as CCl_4 , CH_3CCl_3 , CHCl_3 , C_2Cl_4 , and C_2HCl_3 [e.g. *Helas and Wilson, 1992; Kindler et al., 1995*]. It is believed not to have any significant source from chlorofluorocarbons, which break down to COF_2 or COCIF due to the greater strength of the C-F bond as compared with the C-Cl bond [*Sen et al., 1996*]. COCl_2 has both a tropospheric source (OH-initiated oxidation of these parent compounds) and a stratospheric source (mainly UV photolysis of CCl_4).

Toon et al., *Geophys. Res. Lett.*, **28** (2001) 2835



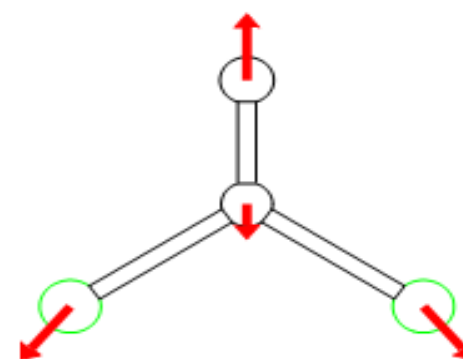
ν_1 (1877 cm^{-1})

A'



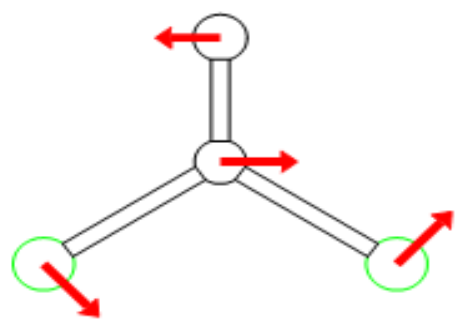
ν_2 (840 cm^{-1})

A'



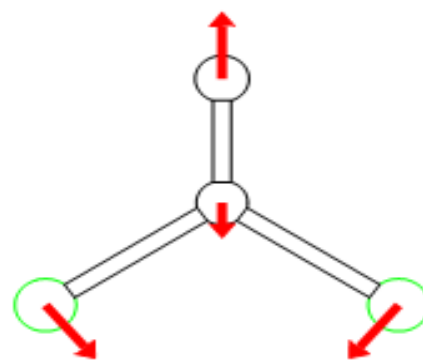
ν_3 (567 cm^{-1})

A'



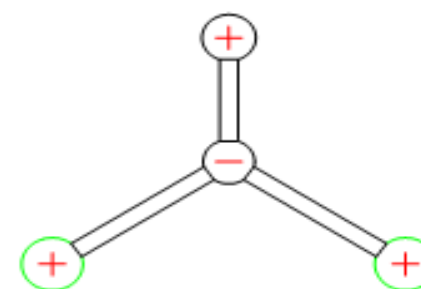
ν_4 (440 cm^{-1})

A'



ν_5 (285 cm^{-1})

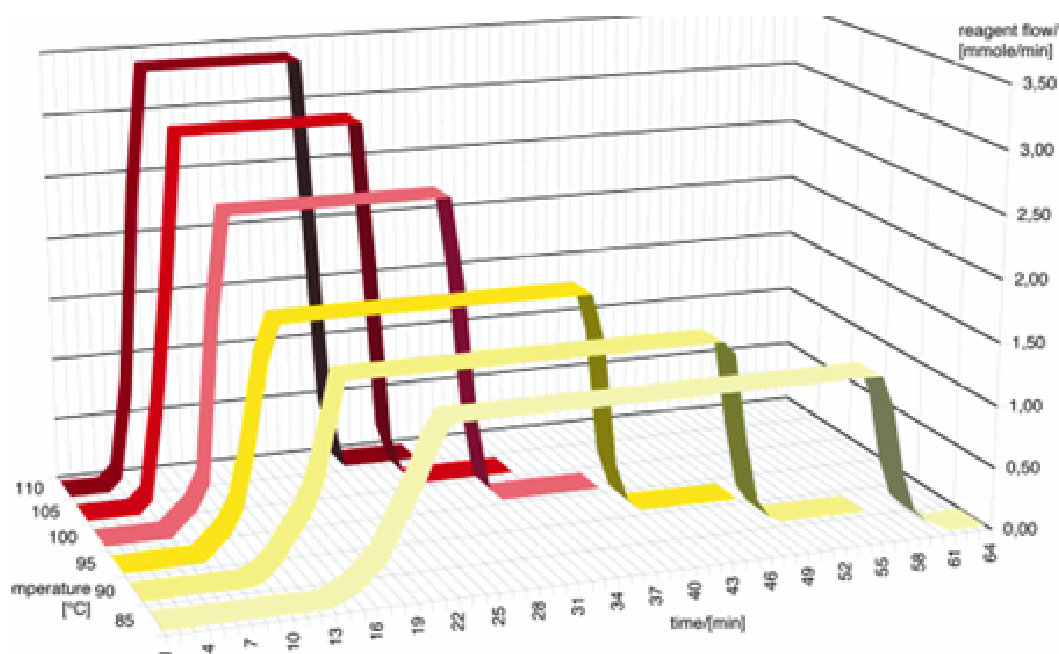
A'



ν_6 (580 cm^{-1})

A''

Phosgene production: Triphosgene was heated to generate phosgene



Phosgene production begins at a temperature of 80°C, below which the gas is not produced. The reaction proceeds cleanly up to 110°C at a steady rate

- The gas is trapped in the liquid nitrogen
- Pumping of the not condensable impurities (CO, CO₂,...)

Homogeneity of the temperature along the entire optical path length

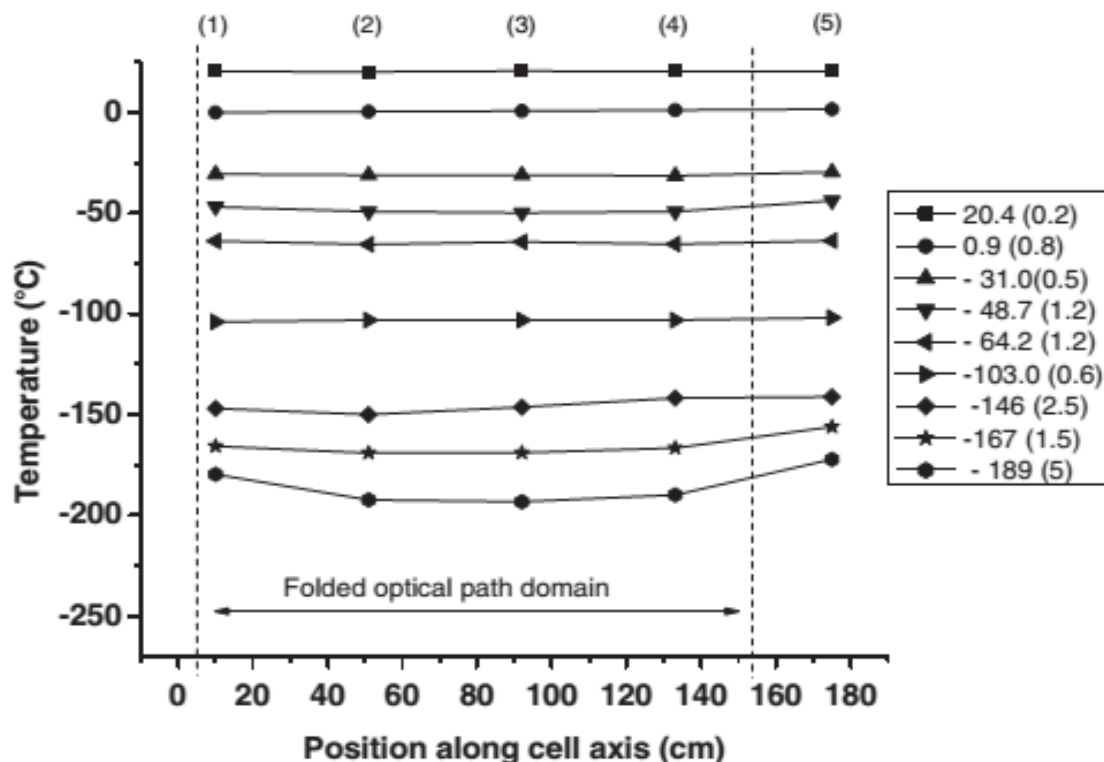


FIG. 5. Temperature (°C) profile vs. position along the cell body for the SOLEIL-LISA Cryocell at nine different cooling temperatures near 293, 274, 242, 224, 209, 170, 127, 106, and 84 K (average temperatures). The temperature sensor indexes are in parenthesis. Sensor 5 is slightly outside the optical path. The numbers on the right indicate average temperatures and 1σ deviations.

Along the cell body five pairs of flexible heaters (500 W, Kapton encapsulated NiCr) were glued with Stycast 2850FT and connected to five separate temperature controllers. This allows a fine adjustment of the temperature and compensations of the small differences between center and extremities of the cell body. The regulation is based on five Pt100 class A temperature sensors, with stated accuracy of $\pm 0.1^\circ\text{C}$